Microscopic model for sequential tunneling in semiconductor multiple quantum wells

Ramón Aguado and Gloria Platero
Instituto de Ciencia de Materiales (CSIC), Cantoblanco, 28049 Madrid, Spain

Miguel Moscoso and Luis L. Bonilla
Escuela Politécnica Superior, Universidad Carlos III de Madrid Butarque 15, 28911 Leganés, Spain

(Received 13 March 1997)

We propose a self-consistent microscopic model of vertical sequential tunneling through multiple quantum wells. The model includes a detailed description of the contacts, uses the transfer Hamiltonian for expressions of the current and it treats the Coulomb interaction within a mean-field approximation. We analyze the current density through a double well and a superlattice and study the formation of electric-field domains and multistability coming from the Coulomb interaction. Phase diagrams of parameter regions (bias and doping in the heterostructure and in the contacts, etc. . . .), where the different solutions exist, are given. [S0163-1829(97)50128-7]

Coulomb interaction in heterostructures with large area wells is a small effect compared with the energy difference between noninteracting eigenstates of the structure. Therefore, a mean-field model gives, for many purposes, a good description of the system. Among features of the transport properties having their origin in Coulomb interaction, intrinsic bistability has great importance. This physical phenomenon arises from the nonlinear effect of the electric charge on the induced electrostatic potential, and it has been predicted and observed in double barrier structures (DB).[1–4] Furthermore, in the presence of a laser polarized in the sample growth direction, additional bistability regions have been theoretically predicted.[5] In this paper, we deal with the statics and dynamics of vertical transport through biased heterostructures whose main mechanism is sequential tunneling. This is a topic that has attracted a great deal of attention in recent times. In weakly coupled superlattices, multistability due to domain formation, has been much studied both theoretically and experimentally.[6–9] When the charge in the superlattice is small due to lower doping in the wells, self-sustained current oscillations and chaos due to domain dynamics are possible.[10–12] So far, the most successful modeling of these phenomena use discrete rate equations for the electron density and electric field in each well, plus constitutive laws for the current, bias, boundary, and initial conditions.[7,8,13] The laws may be phenomenological[8] or obtained from microscopic considerations.[7,14,15] In all cases cited, the boundary conditions were selected in a more or less *ad hoc* manner by using the available information from experiments. This is particularly annoying because the boundary conditions select the relevant dynamics of electric-field domains in the oscillatory regime.[16] In this paper, we present a microscopic model that includes in a natural way boundary conditions due to the emitter and collector regions of a multiwell structure (MW). We then solve it for the cases of a double quantum well (DQW) and a superlattice (SL). The presence of intrinsic bistability is demonstrated through phase diagrams and I-V characteristics obtained by numerical simulation and by means of numerical continuation of stationary solution branches. The main ingredients of our model are as follows: we assume that the characteristic time of intersubband relaxation due to scattering (about 0.1 ps for optical phonon scattering[17]) is much smaller than the tunneling time (less than 0.5 ns), which is in turn much smaller than the dielectric relaxation times responsible for reaching a steady state (about 10 ns for the 9 nm/4 nm GaAs/AlAs superlattices of Ref. 10). This separation of time scales, as well as the configuration of a typical sample allows us to consider that only the ground state of each well is populated and that the tunneling processes are stationary. Our assumptions then justify using rate equations for the electron densities at each well with relations for the currents calculated by means of the transfer Hamiltonian (TH).[18] The rate equations for the electron densities imply that the interwell currents and the currents from the emitter and to the collector are all equal to the total current in the stationary case (a form of Ampère's law may be derived in the time-dependent case). Furthermore, since no current is created or destroyed in the MW, the total charge in it (emitter and collector included) is zero. Finally, the electrostatics is simplified by assuming that the charges are concentrated on two-dimensional (2D) planes located at the wells, emitter and collector regions, as indicated in Fig. 1 and further explained below.

The Hamiltonian for independent electrons in a N-well heterostructure under dc bias is

$$H=\sum_{k_i,\, i\in\{L,R\}} E_{k_i}\mathbf{c}^{\dagger}_{\mathbf{k_i}}\mathbf{c}_{\mathbf{k_i}}+\sum_{i=1}^{N}\sum_{k_i} E_{k_i}\mathbf{d}^{\dagger}_{\mathbf{k_i}}\mathbf{d}_{\mathbf{k_i}} + \sum_{(i,j)\in\{(L,1),(R,N)\}}\sum_{k_i k_j}(T_{k_i k_j}\mathbf{c}^{\dagger}_{\mathbf{k_i}}\mathbf{d}_{\mathbf{k_j}}+\text{H.c.}) + \sum_{i=1}^{N-1}\sum_{k_i k_{i+1}}(T_{k_i k_{i+1}}\mathbf{d}^{\dagger}_{\mathbf{k_i}}\mathbf{d}_{\mathbf{k_{i+1}}}+\text{H.c.}). \quad (1)$$

Here $c^{\dagger}_{k_i}$ (c_{k_i}) are the creation (annihilation) operators in the leads and $d^{\dagger}_{k_i}$ (d_{k_i}) are the creation (annihilation) operators in the wells, and $T_{k_i k_j}$ are the tunneling matrix elements. The latter depend on the local electric field and must be calcu-

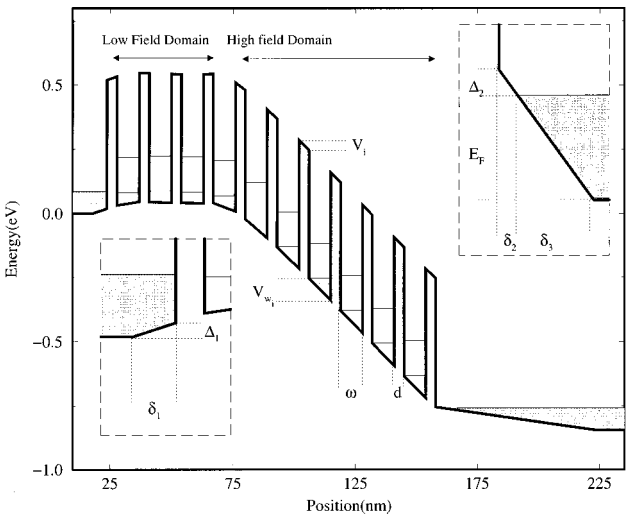

FIG. 1. Electrostatic potential profile in a SL (sample *b*) for $V_2=0.81$ V.

lated self-consistently for each bias. Applying the TH under the assumptions listed before, we obtain the following expressions for the tunneling currents where $J_{e,1}$ and $J_{N,c}$ are the currents in the contacts and $J_{i,i+1}$ the interwell currents:[18]

$$J_{e,1}\equiv J_{0,1}=\frac{ek_BT}{2\pi^2\hbar}\sum_{j=1}^{n}\int A_{Cj}^{1}(\epsilon)B_{1,2}(\epsilon)T_1(\epsilon)\times\ln\left[\frac{1+e^{(\epsilon_F-\epsilon)/k_BT}}{1+e^{(\epsilon_{\omega_1}-\epsilon)/k_BT}}\right]d\epsilon,$$

$$J_{i,i+1}=\frac{e\hbar k_BT}{2\pi^2m^*}\sum_{j=1}^{n}\int A_{C1}^{i}(\epsilon)A_{Cj}^{i+1}(\epsilon)B_{i,i+1}(\epsilon)\times B_{i+1,i+2}(\epsilon)T_{i+1}(\epsilon)\ln\left[\frac{1+e^{(\epsilon_{\omega_i}-\epsilon)/k_BT}}{1+e^{(\epsilon_{\omega_{i+1}}-\epsilon)/k_BT}}\right]d\epsilon,$$

$$J_{N,c}\equiv J_{N,N+1}=\frac{ek_BT}{2\pi^2\hbar}\int A_{C1}^{N}(\epsilon)B_{N,N+1}(\epsilon)\times T_{N+1}(\epsilon)\ln\left[\frac{1+e^{(\epsilon_{\omega_N}-\epsilon)/k_BT}}{1+e^{(\epsilon_F-eV-\epsilon)/k_BT}}\right]d\epsilon. \qquad (2)$$

In these expressions, $i=1,\ldots,N-1$, n is the number of subbands in each well i with energies ϵ_{Cj}^{i} (measured with respect to the origin of potential drops), $B_{i,i+1}=k_i/(w+\alpha_i^{-1}+\alpha_{i+1}^{-1})$ (where k_i and α_i are the wave vectors in the wells and the barriers, respectively; they depend on the local electric field), $T_i(\epsilon)=16k_{i-1}k_i\alpha_i^2e^{-2\alpha_id}(k_{i-1}^2+\alpha_i^2)^{-1}(k_i^2+\alpha_i^2)^{-1}$ is the dimensionless transmision probability through the ith barrier, and w and d are the well and barrier widths, respectively. The spectral functions of the wells are Lorentzians whose widths correspond to the LO phonon lifetimes ($\simeq$1–10 meV): $A_{Cj}^{i}(\epsilon)=\gamma/[(\epsilon-\epsilon_{Cj}^{i})^2+\gamma^2]$ for the ith well. Of course this model can be improved by calculating microscopically the self-energies, which could include other scattering mechanisms (e.g., interface roughness, impurity effects[15]) or even exchange-correlation effects (which affect the electron lifetime in a self-consistent way[19]). We

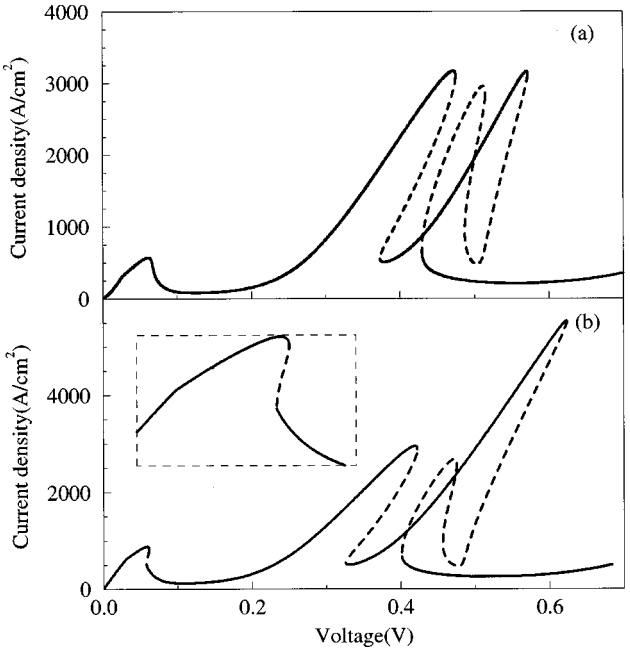

FIG. 2. DQW I-V characteristics (sample *a*). The continuous (dotted) lines correspond to stable (unstable) solution branches: (a) $N_D^W=1.5\times10^{11}$ cm^{-2}; and (b) $N_D^W=4.31\times10^{11}$ cm^{-2}. The inset magnifies the $C1C1$ resonant peak, showing the region of bistability.

have assumed that the electrons in each well are in local equilibrium with Fermi energies ϵ_{ω_i} that define the electronic densities n_i. For a given set $\{\epsilon_{\omega_i}\}$ the densities evolve according to the following rate equations:

$$\frac{dn_i}{dt}=J_{i-1,i}-J_{i,i+1},\quad i=1,\ldots,N. \qquad (3)$$

In these equations $J_{i,i+1}=J_{i,i+1}(\epsilon_{\omega_i},\epsilon_{\omega_{i+1}},\Phi)$, $J_{e,1}=J_{e,1}(\epsilon_{\omega_1},\Phi)$, and $J_{N,c}=J_{N,c}(\epsilon_{\omega_N},\Phi)$, where Φ denotes the set of voltage drops through the structure that are calculated as follows. The Poisson equation yields the potential drops in the barriers, V_i, and the wells, V_{wi} (see Fig. 1):

$$\frac{V_{w_i}}{w}=\frac{V_i}{d}+\frac{n_i(\epsilon_{\omega_i})-eN_D^w}{2\varepsilon}, \qquad (4)$$

$$\frac{V_{i+1}}{d}=\frac{V_i}{d}+\frac{n_i(\epsilon_{\omega_i})-eN_D^w}{\varepsilon}, \qquad (5)$$

where ε is the GaAs static permittivity, $n_i(\epsilon_{\omega_i})$ is the 2D (areal) charge density (to be determined), which is singularly concentrated on a plane located at the end of the ith well, and N_D^w is the 2D intentional doping at the wells. The emitter and collector layers can be described by the following equations:[3]

$$\frac{\Delta_1}{\delta_1}=\frac{eV_1}{d},\quad \sigma=2\varepsilon\frac{V_1}{d}\simeq eN(E_F)\Delta_1\delta_1, \qquad (6)$$

$$\frac{\Delta_2}{e}=\frac{V_{N+1}\delta_2}{d}-\frac{1}{2\varepsilon}eN_D\delta_2^2,\quad \delta_3=\frac{\delta_2E_F}{\Delta_2}. \qquad (7)$$

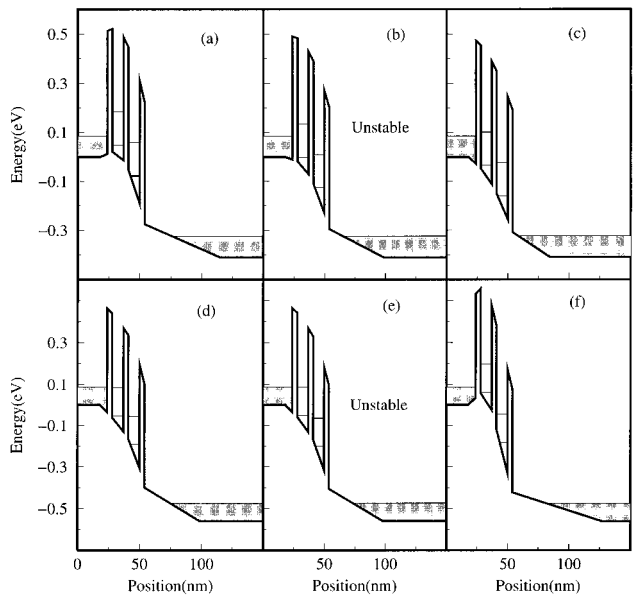

FIG. 3. (a)–(c) The three stationary potential profiles for the DQW structure of Fig. 2(a) at 0.41 V, ordered from highest to lowest current density. (d)–(f) Same for a bias $V=0.56$ V. In all cases the emitter Fermi energy and the subband energies are depicted.

To write the emitter Eqs. (6), we assume that there are no charges in the emitter barrier. Then the electric field across δ_1 (see Fig. 1) is equal to that in the emitter barrier. Furthermore, the areal charge density δ required to create this electric field is provided by the emitter. $N(E_F)$ is the density of states at the emitter E_F. To write the collector Eqs. (7), we assume that the region of length δ_2 in the collector is completely depleted of electrons[3] and local charge neutrality in the region of length δ_3 between the end of the depletion layer δ_2 and the collector. The conditions of global charge conservation and overall voltage bias close the set of equations:

$$\sigma+\sum_{i=1}^{N}\left(n_i(\varepsilon_{\omega_i})-eN_D^w\right)=eN_D\left(\delta_2+\frac{1}{2}\delta_3\right), \tag{8}$$

$$V=\sum_{i=1}^{N+1}V_i+\sum_{i=1}^{N}V_{wi}+\frac{\Delta_1+\Delta_2+E_F}{e}. \tag{9}$$

Note that the right hand side of Eq. (8) is the positive 2D charge density depleted in the collector region. Instead of the rate Eqs. (3), we can derive a form of Ampère's law which explicitly contains the total current density $J(t)$. We differentiate Eq. (5) with respect to time and eliminate n_i by using Eqs. (3). The result is

$$\frac{\varepsilon}{d}\frac{dV_i}{dt}+J_{i-1,i}=J(t),\quad i=1,\ldots,N+1, \tag{10}$$

where $J(t)$ is the sum of displacement and tunneling currents. The time-dependent model consists of the $3N+8$, Eqs. (4)–(10) [the currents are given by Eqs. (2)], that contain the $3N+8$ unknowns $\epsilon_{\omega i}$, V_{w_i}, $(i=1,\ldots,N)$, V_j $(j=1,\ldots,N+1)$, Δ_1, Δ_2, δ_k $(k=1,2,3)$, σ, and J. Thus we have a system of equations that, together with appropriate initial conditions, determine completely and self-consistently our problem. The boundary conditions arise in a natural way. Notice that the charge and electric field at the boundaries cannot be set prior to the calculation of the whole structure, which all previous models did.[7,8,15]

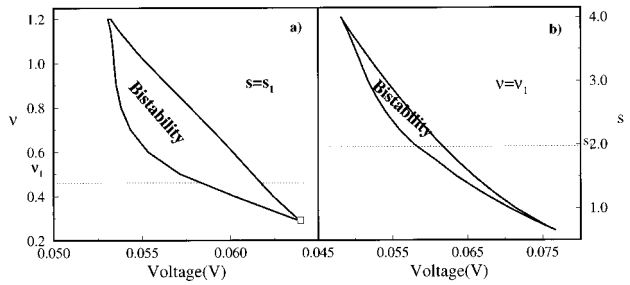

FIG. 4. Phase diagrams showing the regions of multistability for the DQW (sample a): (a) dimensionless well doping ν versus voltage at $s_1=1.97$ ($N_D=2\times10^{18}$ cm^{-3}), $\nu_1=0.46$ corresponds to the well doping of Fig. 2(b); (b) dimensionless contact doping s versus voltage, at ν_1.

In this paper, we are interested in analyzing the statics of the model and the stability of the stationary solutions. One way to do this is to numerically solve the algebraic-differential system (4)–(10) (plus appropriate initial conditions) for each bias until a stationary profile is reached. This procedure misses unstable states and multistability regions require special handling. Thus, we follow this procedure for a given value of the bias and then use a numerical continuation method to obtain all stationary solution branches in the I-V characteristic diagram. This yields both unstable and stable solution branches. Direct integration of the stationary equations [dropping the displacement current in Eq. (10)] presents important problems of numerical convergence to the appropriate solutions in regions of multistability (see below).

We analyze a DQW (sample a) consisting of 90 Å GaAs wells and 40 Å $Ga_{0.5}Al_{0.5}As$ barriers. The doping at both emitter and collector is $N_D=2\times10^{18}$ cm^{-3}, and in the wells it is $N_D^w=1.5\times10^{11}$ cm^{-2}. The half-width of the well states is $\gamma=4$ meV in Eqs. (2) and $T=0$. We do not consider the effect of other symmetry points in the conduction band than Γ. Figure 2 shows the DQW I-V characteristic for two different values of N_D^w. In Fig. 2(a) the low bias peak corresponds to $C1C1$ tunneling (Ci are the conduction subbands ordered starting from that with lowest energy) between adjacent wells. At higher bias multistability of stationary solution branches sets in (three stable solutions coexist at about 0.44 V). To understand the difference between these solutions, we have depicted in Fig. 3 the potential profile of three different solutions (two stable, one unstable) corresponding to the same voltage (0.41 V). In Fig. 3(a), the electrons flow from the emitter to $C1$ in the first well. Then there is $C1C2$ tunneling to the second well. A stable solution with lower current density is shown in Fig. 3(c). There the $C1$ at the first well is below the bottom of the emitter layer, then the electrons flow to $C2$ at the first well instead and J is smaller. A similar situation occurs at higher bias, Figs. 3(d)–3(f). The subbands of the two wells are clearly off resonance for the solution with lowest current, Fig. 3(f). Notice that the current flowing from the emitter to the structure and the potential profile are quite different for the different solutions of our

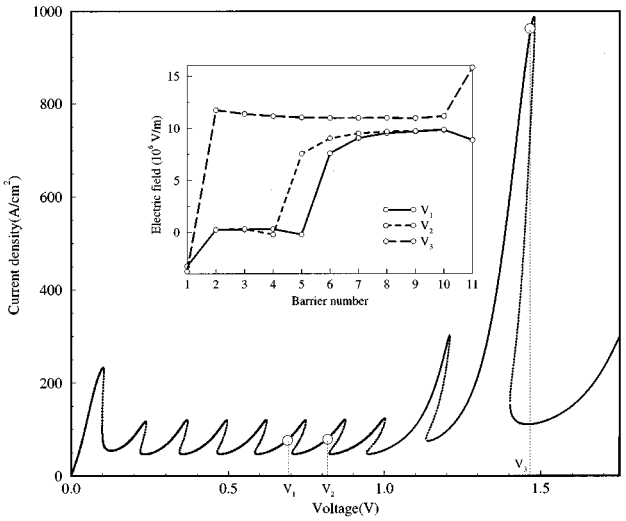

FIG. 5. I-V characteristic curve of a SL (sample *b*). The inset shows the electric field distribution through the SL for three voltages: $V_1=0.69$ V; $V_2=0.81$ V; $V_3=1.48$ V.

model. This shows that boundary conditions assumed in previous publications might constitute gross oversimplifications of the physical situation. In Fig. 4 we present the regions of multistability depending on the bias and the dimensionless doping inside the wells, $\nu=ewN_D^w/[\varepsilon(\epsilon_{C2}-\epsilon_{C1})]$, or at the emitter $s=ew^2N_D/[\varepsilon(\epsilon_{C2}-\epsilon_{C1})]$. We see that there is a lower and upper limit for both ν and s to have bistability. Then it is possible to control the presence and extent of bistability in a sample by changing the doping in the wells or at the contacts and the well widths.

In Fig. 5 we plot the I-V curve of a 90 Å GaAs/40 Å $Ga_{0.5}Al_{0.5}As$ SL with 11 barriers and 10 wells. Its doping is as in Fig. 2(a). The stable branches are shown as continuous lines in Fig. 5. The inset shows three electric field profiles corresponding to three different voltages. They show the presence of domains in the SL with a domain wall that moves one well as we change the bias from one branch to the next one. Domain coexistence is also shown in the SL electrostatic potential profile; see Fig. 1 for a fixed bias $V_2=0.81$ V. The first branch in Fig. 5 corresponds to $C1C1$ tunneling. As V increases, $C1C2$ tunneling becomes possible in part of the structure and we have domain formation. This situation confirms the findings with other discrete models with *ad hoc* boundary conditions.[7–9,13–15] An interesting feature in Fig. 5 is that satellite peaks have a smaller current than the $C1C1$ peak. This agrees with the results of Ref. 15. Another interesting feature due to the voltage drop at the contacts is that the number of branches in the I-V curve is less than the number of wells. This behavior can be understood looking at the branch at 1.21 V, where the low field domain occupies the two wells closer to the emitter. $C1C2$ tunneling occurs between all the wells in the branch with $V_3=1.48$ V corresponding to a very intense peak of the current.

In summary, we have proposed and solved a microscopic self-consistent model for the sequential current through a multiwell structure that includes the current through the contacts and appropriate boundary conditions. We have obtained the static I-V curve and phase diagrams of a DQW and a SL, which display multistability associated to domain formation. Exchange-correlation (not included in our model) has been demonstrated to reduce the bistability in a DB.[19] Including exchange-correlation effects is the aim of a future paper.

We thank M. Kindelan and J. Iñarrea for fruitful discussions and E. Doedel for sending us his program of numerical continuation, AUTO. One of us (R.A.) acknowledges the Fundación Universidad Carlos III de Madrid for financial support. This work has been supported by the CICYT (Spain) under Contract No. MAT 94-0982-c02-02 and by the DGICYT Grant No. PB94-0375, and from the EC Human Capital and Mobility Program Contract No. ERB-CHRXCT930413.

[1] E. S. Alves *et al.*, Electron. Lett. **24**, 1190 (1988).
[2] F. W. Sheard and G. A. Toombs, Appl. Phys. Lett. **52**, 1228 (1988).
[3] V. J. Goldman, D. C. Tsui, and J. E. Cunningham, Phys. Rev. B **35**, 9387 (1987); Phys. Rev. Lett. **58**, 1256 (1987).
[4] T. Fiig and A. P. Jauho, Surf. Sci. **267**, 392 (1992); M. Wagner and H. Mizuta, Jpn. J. Appl. Phys. **32**, 520 (1993).
[5] J. Iñarrea and G. Platero, Europhys. Lett. **33**, 477 (1996).
[6] H. T. Grahn *et al.*, Phys. Rev. Lett. **67**, 1618 (1991).
[7] F. Prengel, A. Wacker, and E. Schöll, Phys. Rev. B **50**, 1705 (1994).
[8] L. L. Bonilla *et al.*, Phys. Rev. B **50**, 8644 (1994).
[9] A. Wacker *et al.*, Phys. Rev. B **55**, 2466 (1997).
[10] J. Kastrup *et al.*, Phys. Rev. B **55**, 2476 (1997).
[11] O. M. Bulashenko and L. L. Bonilla, Phys. Rev. B. **52**, 7849 (1995).
[12] Y. Zhang *et al.*, Phys. Rev. Lett. **77**, 3001 (1996).
[13] L. L. Bonilla *et al.*, SIAM (Soc. Ind. Appl. Math.) J. Appl. Math. **57** (1997).
[14] B. Laikhtman and D. Miller, Phys. Rev. B **48**, 5395 (1993).
[15] A. Wacker and A. P. Jauho, Phys. Scr. **T69**, 321 (1997).
[16] F. J. Higuera and L. L. Bonilla, Physica D **57**, 164 (1992).
[17] F. Capasso *et al.*, Appl. Phys. Lett. **48**, 478 (1986).
[18] M. Jonson, Phys. Rev. B **39**, 5924 (1989); G. Platero, L. Brey, and C. Tejedor, *ibid.* **40**, 8548 (1989).
[19] N. Zou *et al.*, Phys. Rev. B **49**, 2193 (1994).